

Contents lists available at ScienceDirect

Reliability Engineering and System Safety

Journal homepage: www.elsevier.com/locate/ress





Resilience assessment and enhancement evaluation of power distribution systems subjected to ice storms

Guangyang Hou a,*, Kanthasamy K. Muraleetharan a, Vinushika Panchalogaranjan h, Paul Moses \ Amir Javid C, Hussein Al-Dakheeli C, Rifat Bulut C, Richard Campos \ P. Scott Harvey a, Gerald Miller a, Kirby Boldes D, Maha Narayanan B

• School of Civil Engineering and Environmental Science, University of Oklahoma, Nonnan, OK 73019, USA b School of Electrical and Computer Engineering, University of Oklahoma, Nonnan, OK 73019, USA c School of Civil and Environmental Engineering, Oklahoma Stare University, Stillwater, OK 74078, USA

ARTICLE INFO

Keywords: Power distribution systems Resilience assessment Enhancement Ice storms Fragility modeling Vegetation management Tree-induced risk

ABSTRACT

Overhead power distribution systems are very susceptible to ice storms. Each year power outages due to ice storms result in extensive economical loss and restoration costs all around the world. Climate change and aging further highlight the need for resilient power distribution systems against ice storms. This paper proposes a probabilistic framework for assessing and evaluating the enhancements of the ice storm resilience of power distribution systems, with a focus on fragility modeling of power distribution components (i.e., power poles and wires). The framework is able to assess the impact of ice storms on the resilience of power distribution systems and evaluate the cost-effectiveness of resilience enhancement strategies such as upgrading poles and vegetation management. Specifically, the limitations of tree-induced risk assessment in previous studies are overcome by developing fragility models of tree-induced component failures and using an empirical tree damage fragility function. The fragility of distribution components subjected to ice storms is thoroughly investigated by considering four different failure modes and the effect of wind attack angle. The proposed framework is demonstrated with a power distribution network in Oklahoma.

1. Introduction

Electrical power systems are the backbone of modern societies. The functionality of other critical infrastructure systems, such as transportation, water, gas, and communication systems, depends on the reliability of electrical power systems [1]. Therefore, disruption of electrical power systems can cause catastrophic consequences, which is evidenced by recent wide-scale blackouts [2]. Overhead electrical power systems are very susceptible to weather-related events such as hurricanes and ice storms. Power distribution systems usually suffer more damage during weather-related events, as compared to power generation and transmission systems [3]. Approximately 80 to 90% of the power outages that occur in the United States are due to extreme weather-caused disruption of distribution systems [4].

As a severe weather event, ice storms pose a great threat to power distribution systems. An ice storm can cause significant ice accretion on power lines. The ice load, usually combined with strong wind, can snap

power lines and bring down power poles. Additionally, heavy ice load can break trees and tree branches. Falling trees and tree branches can cause further damage to power lines and poles. North American Ice Storm of 1998 damaged large portions of power distribution systems (including at least 26,500 poles) and many transmission towers in Ontario and Quebec [5]. As a result, more than 3.5 million customers in total lost power for up to a month in some areas. October 2020 Ice Storm in Oklahoma destroyed more than 4200 power poles and caused 300, 000 people to be without power [6].

Climate change is expected to increase the frequency and intensity of extreme weather events such as ice storms in the future [7-9]. In addition, aging poses another challenge to infrastructure systems by reducing the strength of infrastructure components [10,11]. These challenges further highlight the need for resilient power distribution systems [12,13]. Although there is no consensus on the definition of resilience, it generally refers to the capacity of a structure or system to survive, adapt, and recover quickly from external disturbances [14-17].

E-mail address: guangyang.hou@ou.edu (G. Hou).

^{*}Corresponding author.

extraordinary and high impact-low probability events such as due to extreme weather, rapidly recover from such disruptive events and absorb lessons for adapting its operation and structure to prevent or mitigate the impact of similar events in the future." Currently, it is difficult for the stakeholders to make rational investments to enhance the resilience of power distribution systems most efficiently and effectively because of the scarcity of risk assessment and impact tools [19]. Grid hardening, a combination of effective strategies used to improve grid robustness, has been proven to be an effective method to boost power system resilience against extreme weather [20,21]. Common grid hardening strategies for power distribution systems include upgrading poles, vegetation management, burying power lines underground, and elevating substations. Among them, upgrading poles has received wide attention in recent years [20,22]. However, research on the effect of vegetation management on resilience enhancement is limited. Ma et al. [23] investigated resilience enhancement of power distribution systems against hurricanes with vegetation management and upgrading poles. A tri-level model was used to minimize the hardening investment and load shedding cost with optimal operation strategies. Tari et al. [24] proposed a resilience enhancement framework for distribution networks against extreme weather events. Vegetation management was employed as one of the network hardening strategies. Optimal components for hardening under a limited budget were identified with a genetic algorithm. However, there are two limitations to these two studies. First, reasonable fragility models of tree damage and tree-induced component failures were lacking. A widely used model for estimating the tree windthrow probability was employed by Ma et al. [23]. However, this model was developed based on damage data of forest trees in a mountain area [25]. It cannot be used to predict tree failures in urban areas where the power distribution systems are located, because of different tree characteristics and environments the trees are exposed to [26]. Moreover, the tree-induced wire failure probability was calculated with a simplified model, which ignores some critical factors, such as the weight of falling tree branches and the configuration of power-wire systems. Second, the vegetation management strategies proposed were not realistic and economical. In these two studies, all trees along a line up to several hundred meters were assumed to pose the same risk to poles and wires and will be trimmed or removed if this line is chosen to be hardened. However, only trees that could potentially interfere with power lines need to be trimmed or removed. Therefore, in order to both realistically assess the tree-induced risk and cost-effectively enhance the system resilience, reasonable tree damage fragility functions, fragility models of tree-induced component failure, as well as a targeted vegetation management strategy that focuses on hazard trees, are needed.

When it comes to power systems, according to Panteli and Mancarella

[18], resilience is defined as "the ability of a power system to withstand

Fragility functions define the relationship between the failure probability of a system component and the intensity of a hazard [27]. Under a specific hazard scenario, fragility functions can be used to determine the damage state of each component and further evaluate the system performance. Therefore, fragility functions play an important role in risk analysis and resilience assessment. Many studies have been conducted on the fragility modeling of power distribution components. Empirical fragility curves of electrical overhead lines were generated based on wind-related electrical failure datasets by Dunn et al. [28]. However, empirical approaches are critically dependent on the sufficiency of data. Insufficient data can lead to poor accuracy in fragility modeling. Therefore, fragility modeling with simulation-based approaches is becoming more and more popular. Simulation-based fragility modeling approaches, which often combine Monte Carlo simulation and structural analysis, are able to capture the effect of key design variables such as wind attack angle, wind speed, class, age, pole height and wire size [22,29-31].

Despite the progress made in fragility modeling of power distribution components, more efforts are still needed to fill the research gap as follows. First, previous studies on fragility modeling of power

distribution components mainly focused on extreme winds (e.g., wind storms and hurricanes) without paying attention to ice storms. This can possibly explain the scarcity of ice storm resilience assessment framework of power distribution systems. Fragility models under ice storms and extreme winds cannot replace each other. Because of different loading conditions, not only structural analysis models but also fragility curve formulae are different. For example, the power-wire system model can better reflect the 3D behaviors of power poles and wires during ice storms than the widely used individual pole model subjected to hurricanes [30,32]. In addition, the hazard intensity in the ice storm fragility functions is characterized by two measures (i.e., ice thickness and wind speed), as compared to one measure (i.e., wind speed) in the hurricane fragility models. Second, failure modes of power distribution components were not fully captured in previous fragility models. In previous studies, bending failure of poles is assumed to be the only failure mode. Wire breakage is ignored, although evidences show its occurrence during hurricanes and ice storms [7]. This is partly due to the limitation of the individual pole model, in which the wires are not included. Neglecting this failure mode can lead to an underestimation of the ice storm risk posed to power distribution systems. In addition, faults or damages induced by falling tree branches have not been fully addressed although trees have been recognized as the most destructive cause of power outages [33]. According to Wang [34], there are four typical tree-caused faults of overhead lines: (1) pole failure; (2) wire breakage; (3) short circuit fault which occurs when a bridge is formed between wires by falling trees; (4) short circuit fault which occurs when wires are pushed together by falling trees. These failure modes caused by falling trees need to be included in the fragility model to realistically assess the ice storm risk. However, only pole failure caused by falling trees was investigated by Yuan et al. [31]. The other three failure modes have not been addressed. Third, the effect of wind attack angle was not considered in most fragility models. Previously, the worst scenario was assumed in which wind is perpendicular to power lines. This assumption will obviously lead to an overestimation of the failure probability of poles and wires when the wind is not perpendicular to power lines. For example, if the wind is parallel to the power lines, there will be no wind load on the wires because the frontal area is zero. Although the effect of wind attack angle was considered in the work of Darestani and Shafieezadeh [29], only pole failure induced by winds was considered in their fragility models.

To address the aforementioned limitations regarding vegetation management and component fragility, this paper proposes a probabilistic framework for assessing and enhancing the ice storm resilience of power distribution systems, with a focus on fragility modeling of power distribution components. The proposed resilience framework includes five components: hazard characterization, component fragility, power distribution system performance, system restoration, and resilience enhancement evaluation. The framework is able to assess the impact of ice storms on the resilience of power distribution systems and evaluate the cost-effectiveness of resilience enhancement strategies. Specifically, the limitations of tree-induced risk assessment in previous studies are overcome by developing fragility models of tree-induced component failure and using reasonable tree damage fragility functions. The fragility of distribution components subjected to ice storms is thoroughly investigated by considering four different failure modes and the effect of wind attack angle. A power distribution network in Oklahoma is used to demonstrate the effectiveness of the proposed framework. The effects of ice storm intensity, wind direction, and recovery resources on the system resilience are investigated in the demonstrative study. Moreover, the cost-effectiveness of different grid hardening strategies is studied by considering investment budget and power outage cost.

The primary contributions of this paper include (1) developing a probabilistic framework for assessing and evaluating the enhancements of the ice storm resilience of power distribution systems; (2) developing fragility models of PDS components subjected to ice storms; three failure modes of PDS components induced by trees, ice, and wind, are

investigated for the first time; and (3) thoroughly investigating the impact of tree failures on the PDS resilience by developing fragility models of tree-induced component failures and using an empirical tree damage fragility function.

The rest of this paper is organized as follows. In Section 2 the probabilistic power distribution resilience enhancement framework is described. In Section 3 the fragility modeling of power distribution components is presented. In Section 4 the framework is demonstrated with a power distribution network. In Section 5 results are summarized and conclusions are provided.

2. Resilience enhancement framework of power distribution systems against ice storm

A probabilistic framework is proposed to assess and enhance the resilience of power distribution systems subjected to ice storms, which includes five parts: ice storm characterization, component fragility model, power distribution system performance model, system restoration model, and resilience enhancement evaluation, as shown in Fig. 1. First, an ice storm scenario is generated and characterized with several key hazard intensity measures, such as ice thickness, wind speed, and wind direction. Second, based on fragility models of power distribution components, the possible damage state of each component can be estimated for a given ice storm scenario. Third, the performance of the impacted power system is evaluated with a connectivity-based approach. Fourth, each failed component in the system is repaired with a probabilistic restoration model. Finally, the system resilience is enhanced with a cost-effective targeted hardening method, with which components with high resilience achievement worth are given high hardening priority. The details of each component in the framework are elaborated below.

2.1. Ice stonn characterization

Deterministic ice storm scenarios are used in this study, which are characterized by deterministic ice thickness, wind speed, and wind direction. Meanwhile, it is assumed that the power distribution system is exposed to the same weather condition during an ice storm. This means that the ice thickness, wind speed, and wind direction are the same over the entire distribution system. This assumption is valid because distribution systems usually cover a small geographical area [18]. An ice storm weather model can simulate more realistic ice storm events temporally and spatially. However, doing so is beyond the scope of this paper, but the framework is flexible enough to incorporate predictions from such a weather model.

2.2. Component fragility model

Ice storms can damage different power distribution components in different ways. This paper considers the poles and wires because they are the most critical and vulnerable components in distribution systems [35]. During past ice storm events, poles and wires were damaged by either the ice and wind directly or falling tree branches indirectly [6,34]. Therefore, two scenarios are considered in the component fragility models. In scenario 1, two failure modes including pole failure and wire

breakage caused by the combined effect of ice and wind are considered. In scenario 2, the other two failure modes including wire breakage and short circuit caused by ice and falling trees are considered. It is noted that pole failure is not identified for the tree-ice scenario in this study. Normally, a distribution network includes 1-phase and 3-phase lines. For a 3-phase line system, it is assumed a short circuit will occur once a tree branch falls on it. In this case, a bridge between different wires is easily formed because these wires are in an approximately horizontal plane. In contrast, for a 1-phase line system, a short circuit is assumed to occur if the top wire contacts the underslung neutral wire under the weight of tree branches and ice. Therefore, fragility models of wire breakage and short circuit will be developed for the 1-phase power line for the tree-ice scenario. Those component fragility models will be developed with a simulation-based approach based on finite element analysis and Monte Carlo simulation. Various factors such as phase type, pole class, and wind attack angle are also considered. The details of component fragility models will be provided in Section 3. It should be noted that the fragility of different components under different scenarios is assumed to be independent. This assumption has been adopted in many previous studies [1,23,36].

With developed fragility functions, the failure probability of distribution components such as poles and wires for given hazard intensities (e.g., wind speed, ice thickness, and tree weight) can be calculated. Specifically, the failure probability of pole i can be computed by:

$$Pc, Pole, i = Pbd, iw, i$$
 (I)

where Pl,d,iw,i is the bending failure probability of pole i due to ice and wind load. The failure probability of wire **j** can be calculated by:

$$p_{f,\text{wire},j} = \max(p_{\text{br},\text{iw},j}, p_{\text{tree},j}p_{\text{br},\text{ti},j}, p_{\text{tree},j}p_{\text{st},\text{ti},j})$$
(2)

where Pbr,iwj is the breakage probability of wire *j* due to ice and wind load; Pbr,tij and P_st,tij are the breakage and short circuit probability of wire *j* due to falling trees and ice load, respectively; Ptreej is the damage probability of trees along wire *j*, which can be calculated by:

$$Pt=$$
; = I - (! - $Pt=$,iw)" (3)

where Ptree, iw is the tree damage probability due to ice and wind load, which is provided by tree damage fragility function; n is the number of hazard trees along wire j. In this study, the empirical tree damage fragility functions are derived based on tree damage data following an ice storm that struck Oklahoma in October 2020.

2.3. System perfonnance model

The radial system is the most common type of power distribution system in the US [31]. The radial distribution system has a tree configuration. In distribution systems, protective devices such as switches, fuses, reclosers, and circuit breakers are used to protect circuits from extreme voltages or currents. When a short circuit fault or structural failure occurs, the power in the downstream branches will be completely cut off by the closest protective device in the upstream branch. Therefore, a connectivity-based method is used to estimate the number of customers with power. First, a distribution system is defined

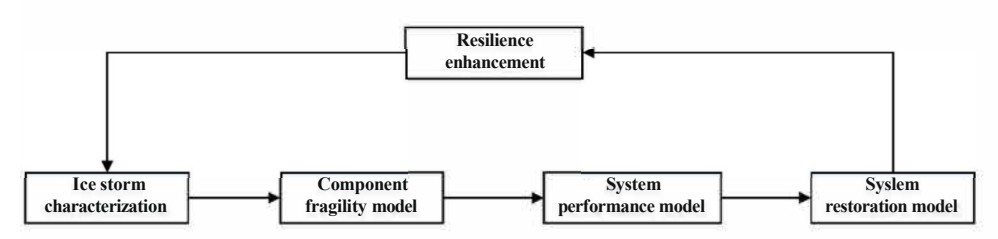


Fig. 1. Resilience enhancement framework.

as a network including nodes and edges, which represent poles and wires, respectively. Each path that connects a customer and the substation is identified, which includes a set of nodes and edges. Second, the protective devices that affect the power flow of each path are identified. If at least one of these devices is open, the path is disconnected. Third, components (poles and wires) that can trip each protective device are identified. If at least one of these components fails, the protective device is opened. Finally, the state of each protective device is determined based on the component failures, which are then used to determine the connectivity of all paths. Once the connectivity of all paths is known, the performance of a distribution system, which refers to the ratio of customers with power, can be evaluated with the following equation:

$$\underline{Q}(\theta) = \frac{\text{No}(t)}{N} \tag{4}$$

where Q(t) is the system performance at time t_i N₀(t) is the number of customers with power at time t_i **N** is the total number of customers.

2.4. System restoration model

When a component failure occurs, the power distribution system needs to be restored as fast as possible so that the loss can be minimized. Restoration activity may include replacement of damaged poles and wires and removal of tree branches that fell. Regarding the restoration process, two factors need to be considered: restoration resources and repair sequence. In this paper, the restoration resources refer to the number of repair teams, consisting of repair crews, equipment, and material. It is assumed that a failure only requires one repair team for the restoration [1]. In addition, the restoration time of different component failures is assumed to follow a normal distribution [1,35]. According to Ouyang and Duenas-Osorio [35], the restoration time (in hours) for a pole failure, a wire failure, and a tree-induced short circuit has the distribution $t_{i,ow}$ N(5, 2.5), $l_{conductor}$ N(4, 2.5), and t,1wrt N(1, 0.5), respectively. To maximize the overall performance of power distribution systems during the restoration process, restoration priority should be given to the critical components connected to the greatest number of customers. In this study, the criticality of components is measured with a critical index (CD, which is defined as the change in system performance (i.e., the number of customers with power) when the component is removed from the system. Component CI can be calculated with the following equation:

$$Cl;=1-Q(.5;=1)$$
 (5)

where 8_i is the state indicator of component i, if component i fails, $8_i = 1$ or else $8_i = 0$; 0 (\clubsuit 1) is the system performance when only component i fails but others still operate. All components are ranked based on their CI. Repair teams are assigned to repair components based on ranking. Typically, components on the mainline and close to the substation have relatively high rankings and high recovery priority. The restoration is a time-dependent process. During the restoration, once a component is repaired, the system performance is updated. This process continues until all failures are repaired and the system recovers to normal operating conditions. For an ice storm event, the resilience of a power distribution system can be evaluated with the following equation [1]:

$$RI = \frac{J_{c}^{\prime 0 + lc} Q(t) dt}{tc}$$
 (6)

where RI is the resilience index; to is the time when the power network is hit by the ice storm; tc is the control time for the period of interest. The power outage cost during an ice storm can be calculated with the following equation:

$$C_{p} = Lc;P;,,$$

$$U_{p} = Lc$$

where C_p is the power outage cost; Ci is the unit cost of lost load to customer i; P_{ij} , is the lost load of customer i at time t.

2.5. Resilience enhancement evaluation

In this study, upgrading poles and vegetation management are employed to improve the resilience of distribution systems against ice storms. Upgrading poles refers to replacing poles with higher classes. Vegetation management refers to trimming or removing hazard trees near the overhead power lines to reduce the chance of interference. It is assumed that the tree-induced failure risk of a power line reduces to zero after implementing vegetation management. When the investment budget is limited, cost-effective targeted grid hardening is needed. The targeted grid hardening strategy involves not only hardening components that contribute more to the system resilience enhancement, but also reducing the investment cost [21]. In this study, the resilience achievement worth (RAW) index is used to determine the relative importance of each component [21]. RAW provides the increase in system resilience when a component is made 100% robust, which is defined as follows:

$$RAW = \frac{R/(8:=0) - RI}{RI}$$
 (8)

where RI is the actual resilience index during an ice storm event; RI(8; = 0) is the resilience index when component I is made 100% robust during the event. With the targeted hardening strategy, components with higher RAW will be hardened first, until the investment budget is reached.

3. Fragility modeling of distribution components

3.1. Design parameters

Fragility analyses are performed for distribution components including 10,060 poles in the Oklahoma area. This study focuses on two commonly used pole types in this area, including 1-phase and 3-phase line poles, which are shown in Fig. 2. In addition, for both 1-phase and 3-phase line poles, Classes 2, 4 and 5 are much more prevalent than other classes. Therefore, fragility analysis is performed for these three pole classes. To characterize a large number of components in terms of geometry and material property, both deterministic and stochastic parameters are needed, because some parameters have very negligible uncertainty and others have high uncertainty [37]. For most stochastic parameters related to geometry and material property, lognormal or normal distribution functions are fitted to the data. Table 1 gives the deterministic and stochastic parameters. Based on the height data, pole height for a certain class can be classified into 3-4 groups; therefore, the discrete probability distribution is used to describe the height. The pole diameter for a given height and class is then determined based on ANSI 05.1 [38]. The poles are made of Southern Pine. The span length of power lines vary significantly, which follows a normal distribution. Aluminum Conductor Steel Reinforced (ACSR) is used for both phase and neutral wires. The density, diameter, and breaking strength of ACSR wires follow lognormal distributions, with their COV greater than 0.2. A deterministic elastic modulus of 81 GPa is used for ACSR wires [39]. Due to the lack of design details of crossarrns, fiberglass crossarrns used by Yuan et al. [31] are used in this study.

3.2. Applied load

This paper aims to develop fragility functions of distribution components during the ice-wind and tree-ice scenarios. For the ice-wind scenario, both ice and wind loads are applied to poles and wires. According to NESC [40], the wind pressure $P_{\rm w}$ can be calculated with the following equation:

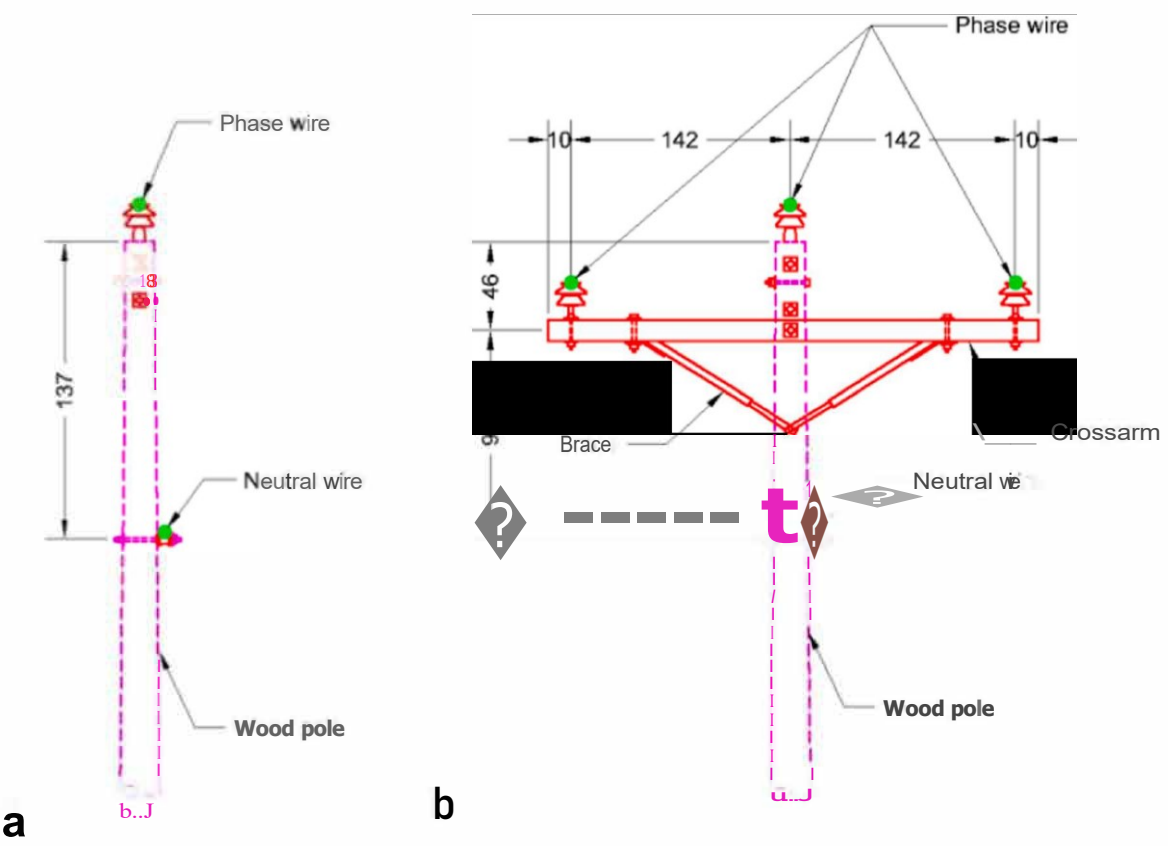


Fig. 2. Distribution pole layout (Unit: cm) (a) 1-phase line pole and (b) 3-phase line pole.

Table 1
Statistics of parameters used in fragility modeling.

Parameter	Probabilistic Model	Mean	COY	Sources
Span (m)	Normal	63.72	0.433	Networl data
Height of each pole class (m)	Discrete probability distribution	120	(1)	Networl data
Fiber strength (MPa)	Lognormal	55.2	0.169	[38]
Wood density (kg/m³)	Normal	500	0.04	[31]
Wood elastic modulus (GPa)	Lognormal	14.68	0.04	[38]
Density of ACSR wire (kg/m³)	Lognormal	3131.2	0.203	Networl data
Diameter of ACSR wire (mm)	Lognormal	7.29	0.240	Networl data
Breaking strength of ACSR wire (MPa)	Lognormal	406.5	0.247	Networ data
Force coefficient	Normal	1	0.12	[31]
Gust effect factor of pole	Normal	0.97	0.11	[31]
Gust effect factor of wires	Normal	0.88	0.11	[31]
Exposure coefficient of pole	Normal	1	0.06	[31]
Exposure coefficient of wires	Normal	1.1	0.06	[31]
Pole diameter (mm)	Deterministic for each class	2	20	[38]
Elastic modulus of fiberglass crossarm (GPa)	Deterministic	75.84	(5)	[31]
Elastic modulus of ACSR wire (GPa)	Deterministic	81		[39]
Density of fiberglass crossarm (kg!m³)	Deterministic	2768	(*)	[31]

Note: network data refers to the data of a power distribution network including 10,060 poles used in this paper.

$$P_{w} = 0.5\rho_{a}k_{z}GC_{f}U_{p}^{2} \tag{9}$$

where P_a is the air density; k_z is the velocity pressure exposure coefficient; G is the gust response factor; C_1 is the force coefficient; U_p is the projected 3-s gust wind speed. It is noted that the projected 3-s gust wind speed U_p is equal to 3-s gust wind speed U for poles. Parameters in Eq. (9) such as the velocity pressure exposure coefficient, the gust response factor, and force coefficient have uncertainties. The probability distributions of these uncertain parameters used in this study are also summarized in Table 1. Because wires are only subject to the wind component in the perpendicular direction, the projected 3-s gust wind speed U_p for wires is equal to $U_p = Usin(a)$, where u is the wind attack angle. Subsequently, the wind load on wires or poles per unit length v0 can be calculated from the following equation:

$$F_w = P_w(D + 2t_i) \tag{10}$$

where D is the wire diameter or pole diameter; ti is the ice thickness.

It is noted that the ice load on the pole is neglected because of its insignificant effect. Therefore, the ice load per unit of wire length Fi can be calculated with the following equation:

$$F_i = 0.25\pi \rho_i \left[(D_c + 2t_i)^2 - D_c^2 \right] \tag{11}$$

where P; is the ice density; $D_{\rm e}$ is the wire diameter. It also should be noted both wind and ice loads are uniformly distributed loads along wires. For the tree-ice scenario, both ice load and the weight of the falling tree branch are applied to wires. The ice load on wires is again calculated with Eq. (11). The weight of the falling tree branch is modeled as a point load at the middle span of the wires, which represents the most unfavorable scenario.

3.3. Finite element analysis

According to Yuan et al. [31], a typical 3-span power-wire system is modeled in ANSYS, as shown in Fig. 3. There are three spans of power lines and four poles in the model. Two guy wires are used to support two end poles. Fixed boundary conditions are applied to the bottom of the poles and guy wires. Poles, crossarms, and braces are modeled with the Beam 4 element. Power lines and guy wires are modeled with the Llnk 8 element. The initial tension in power lines controls the sag and shape of power lines under the self-weight condition. According to Ausgrid [41], when the power line span is between 30 m and 90 m, the recommended stringing tension is 6% of the rated tension strength. Therefore, this criterion is used in the finite element analysis considering that the mean span length is 63.72 m. A two-step nonlinear static analysis is performed to determine the response of the power-wire system during the ice-wind and tree-ice scenarios. Firstly, the initial shape of a power-wire system for a given initial tension and self-weight is determined through a shape-finding analysis. Then, external loads such as wind, ice, and tree are applied to the deformed structure, and the solutions are obtained with the geometric nonlinear analysis. It should be noted only the force and displacement results of the middle span are used for the fragility analysis. This is because two side spans serve as boundary conditions through balancing the load transmitted from the middle span.

3.4. Limit state functi.on

As mentioned above, four failure modes including pole failure, ice and wind-inducted wire breakage, tree and ice-induced wire breakage, and short circuit of wires have been identified and will be investigated with fragility analysis. Pole failure occurs when the maximum stress U_{max},p due to external loads exceeds the fiber strength of poles UJ· The limit state function for the pole failure fragility analysis is given as follows: &, = Uf - U_{max},p• Wire breakage occurs when the maximum stress U_{max},c is larger than the breaking strength of wires ub, The limit state function for the above-mentioned two wire breakage failure modes is given by: & = ub - U_{max},c• Short circuit of the I-phase power system due to falling trees occurs when the phase wire is close enough to the neutral wire under the weight of falling trees. The limit state of the short circuit can be expressed as: $g_n = dp_n - do$, where dp_n is the distance between the phase wire and neutral wire under the tree load; do is the distance threshold that, if exceeded, can cause a short circuit, which is assumed to follow a normal distribution do N(O, 0.1 m).

3.5. Fragility analysis approach and results

A simulation-based approach, which combines finite element analysis and Monte Carlo simulation, is used to develop fragility functions of power distribution components. For a given phase type and pole class, the Latin Hypercube sampling method is used to generate 3000 samples of various design parameters related to demand and capacity, which are the input for finite element analyses with ANSYS. With structural

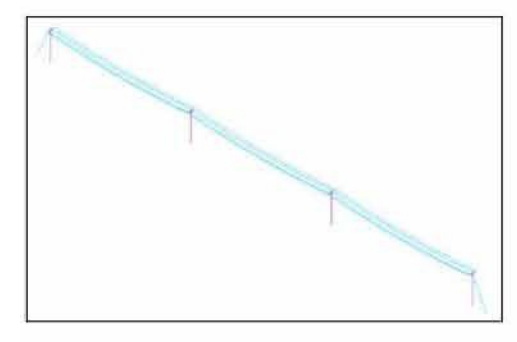


Fig. 3. Finite element model of a 3-span 3-phase power-wire system.

response obtained from finite element analysis, the limit state functions are checked, and the failure probability is calculated after 3000 Monte Carlo simulation runs. Fragility functions are developed after covering a wide range of hazard intensity such as wind speed, ice thickness, and weight of falling tree branches. In the fragility analysis, the ice thickness ranges from 0.635 to 3.81 cm, and the concurrent wind speed ranges from 12.5 to 40 m/s, which are consistent with those with a 500-year mean recurrence interval specified in ASCE 7-16 [42]. As mentioned previously, fragility of distribution components is dependent on several key parameters such as phase type, pole class, wind attack angle, wind speed, ice thickness, and weight of falling trees, so parameterized fragility functions are developed.

3.5.1. Fragility results for the ice-wind scenario

Fig. 4 shows fragility surfaces of the I-phase power system with Class 4 poles under a wind attack angle of 90°. It is found that probabilities of pole failure and wire breakage increase with the increase in wind speed and ice thickness. By comparing different failure modes of the I-phase system, it is found the probability of pole failure is lower than that of wire breakage for a given wind speed and ice thickness. Although the results are not shown here, the 3-phase system has a higher pole failure probability, as compared to the I-phase system. Since there are 2 more phase wires on the 3-phase system, the ice and wind load acting on the system is larger, which leads to larger bending and axial stresses in poles and in turn higher vulnerability.

Fig. 5 shows the fragility curves of the 3-phase system with different pole classes under a wind attack angle of 90°. As shown in Fig. 5(a) and (b), the probability of pole failure and wire breakage for different pole classes increases as the wind speed and ice thickness increase. By comparing the failure probability of different classes, it can be seen that the pole failure probability increases with the increasing pole class. Because poles with higher classes have smaller diameters, they suffer higher stresses under the same loading condition. However, the wire breakage probability decreases as the pole class increases. This can be explained by larger sag and smaller tension in wires with high-class poles due to lower bending stiffness. Under the same loading conditions, larger displacements are generated for high-class poles in lateral and vertical directions because of lower bending stiffness. Since poles provide boundary conditions for wires, larger displacements at the fixed points of poles increase the sag of loaded wires. This in tum leads to decreased tension force in the wires. Therefore, wires with high-class poles are less vulnerable to breakage than those of low-class poles because of smaller tension. This effect becomes more significant under high wind speed and large ice thickness because of the geometric nonlinearity of cable structures. In addition, because the bending stiffness of Class 4 and 5 poles are relatively close, wire breakage probabilities for these two classes are very close.

Fig. 6 presents the fragility curves of the 3-phase system with Class 2 poles under different wind attack angles. It is found in Fig. 6(a) and (b) that, except for some special cases, the probability of pole failure and wire breakage increases with the increase in wind speed and ice thickness. When the wind attack angle is 0°, the frontal area of wires is 0, and there is no wind load acting on wires. Therefore, the wire breakage probability is independent of the wind speed in this situation, as shown in Fig. 6(a). In addition, it can be seen from Fig. 6(b) that pole failure probability is O for different ice thicknesses. This is because the pole is only subject to longitudinal wind load in this situation, which can be balanced by adjacent spans. As a result, the bending stress in poles is relatively low, making it hard to fail. By comparing failure probabilities for different wind attack angles, as the wind attack angle increases, because of increased wind loads acting on wires, the probability of pole failure and wire breakage increases.

3.5.2. Fragility results for the tree-ice scenario

Fig. 7 provides fragility surfaces for the I-phase system with Class 4 poles. It is interesting to find that the probability of short circuit

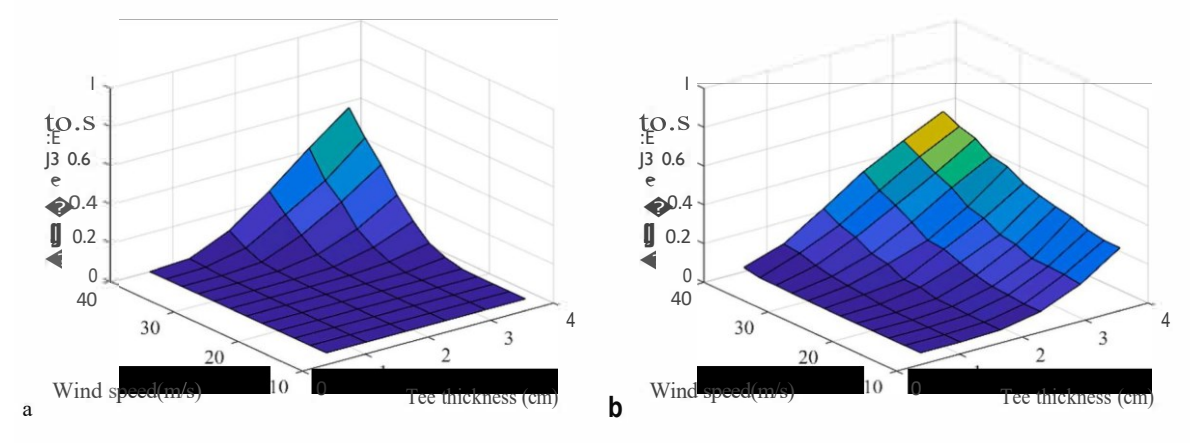


Fig. 4. Fragility surfaces of the 1-phase power system: (a) pole failure; (b) wire breakage.

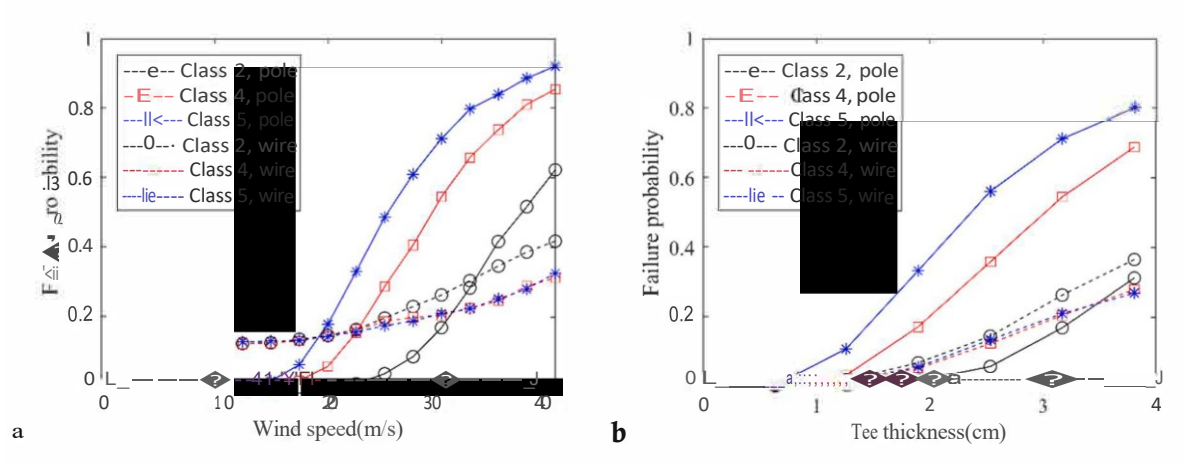


Fig. 5. Fragility curves for different pole classes: (a) = 3.2 cm; (b) U = 30 m/s.

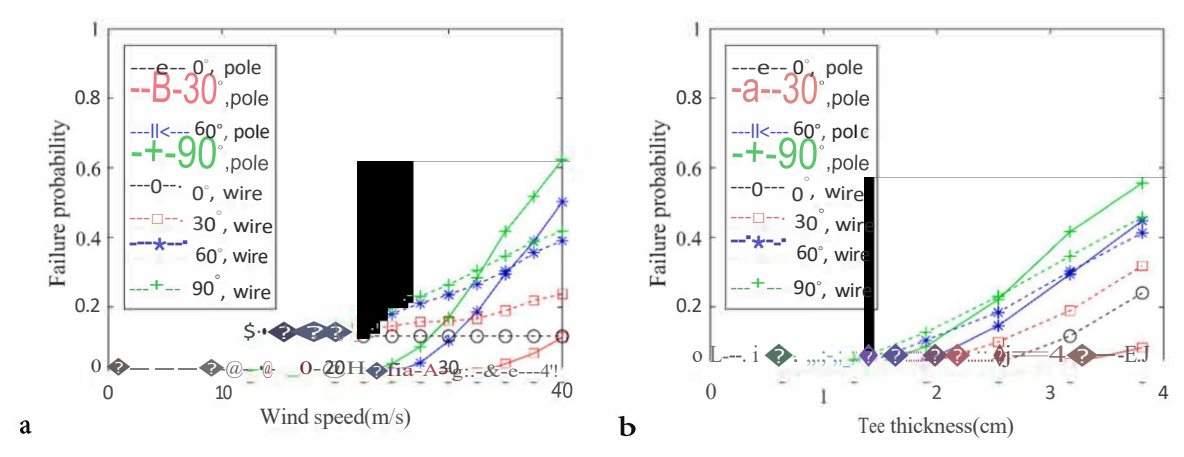


Fig. 6. Fragility curves under different wind attack angles: (a) = 3.2 cm; (b) U = 35 m/s.

increases with the increase in the weight of falling trees but decreases with the increase in the ice thickness. This can be explained by the gravity stiffness effect. The gravity stiffness of a wire reflects its capability to resist vertical deformation, which depends on the load (especially distributed load) acting on it [43]. Considering that the phase wire above and neutral wire below have the same ice load condition, and the short circuit is determined by the tree load-caused deformation, we can assume that the distributed ice load is applied to the phase wire first, followed by the concentrated tree load. A larger ice load leads to higher wire stiffness. This results in a smaller vertical displacement of the phase wire due to the tree load. Therefore, the short circuit probability is lower

for larger ice thicknesses. However, a larger concentrated tree load produces a larger displacement of the phase wire for a constant wire stiffness. This explains why the short circuit probability increases with the increasing tree load. By comparing two different failure modes, it is found that the short circuit dominates the wire failure when the ice thickness is relatively small, whereas the wire breakages are more dominant when the ice thickness is large.

4. Demonstrative example

To illustrate the proposed resilience framework, a power distribution

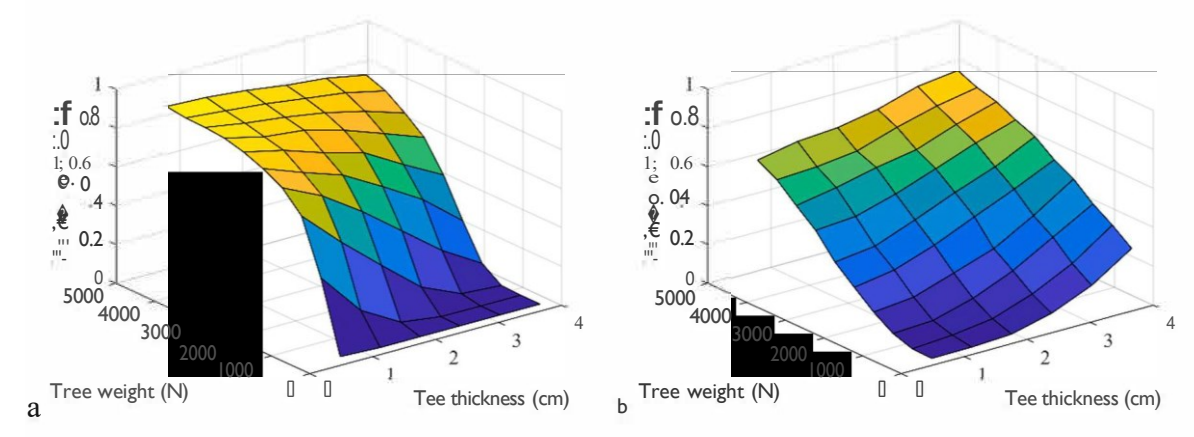


Fig. 7. Fragility surfaces for the tree-ice scenario: (a) short circuit; (b) wire breakage.

network in Oklahoma is utilized in this study. The distribution network is located outside of a town in Oklahoma. This area is an open terrain with scattered obstructions (e.g., buildings, trees) having heights generally less than 9.1 m; the wind exposure category of power poles and lines in this area is C as specified in ASCE 7-16. Fig. 8 shows the layout of the power distribution network, which consists of 770 wood poles and 769 power lines. Power lines with different numbers of hazard trees are displayed in different colors in the figure. Hazard trees are identified with Google Earth, based on the tree size and the distance between the tree and power line. There are three pole classes: Class 2, 4 and 5, accounting for 30.5, 64.9 and 4.6 of the total number of poles, respectively. The substation is located at the northernmost part of the network. In addition, there are many protective devices in the network

such as switches, fuses, line sectionalizers, reclosers, and circuit breakers, although they are not shown in the figure. Other network data includes power line phase, power line direction, and pole class.

The tree failure function is developed by identifying the tree damage during a past ice storm event. Datasets include satellite images of 10 counties in Oklahoma with varying ice accretion levels during the October 2020 ice storm. A random forest supervised classification method is used to process the satellite images before and after the ice storm and detect the change in tree cover caused by the ice storm. Based on the analysis results, the tree cover change, or the tree damage probability Ptree,iw can be expressed as a function of the ice thickness t; (Unit: cm), Ptree,iw = 0.125 + 0.IOIt;. The application range of the tree failure function is 0.25 to 3.8 cm. It was found that the wind had very

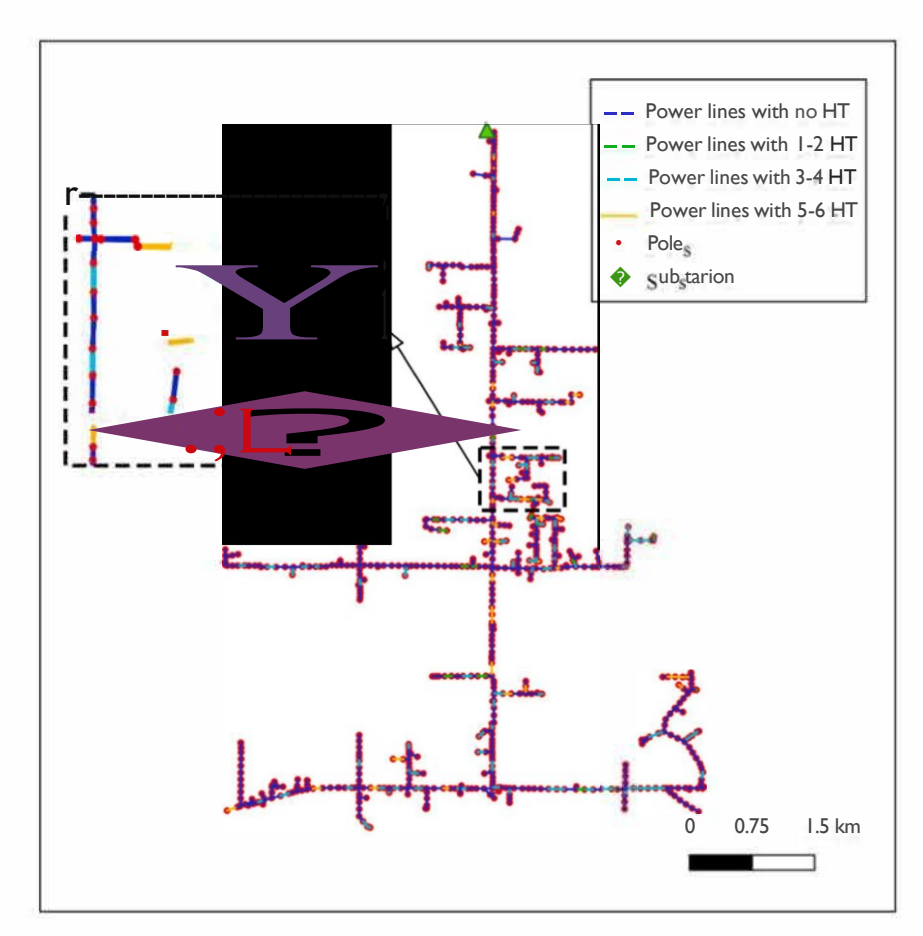


Fig. 8. A power distribution network in Oklahoma (Note: HT refers to hazard trees).

little contribution to the tree cover change during this event. On the one hand, it was because the datasets from a single ice storm event were small. On the other hand, it was because the wind during this ice storm was not very high, with a maximum wind speed of 15.2 m/s. The weight of falling branches is derived from the load causing bending failure of primary branches by realizing that the bending failure normally occurs near the branch attachment to the tree trunk. The following equation is used: $W_{,,..} = 5f''_{,,..}$ where Sis the section modulus of the section near the branch attachment to the tree trunk, S = 3 **d** is the branch diameter; **L** is the distance between the center of gravity of the branch and the branch attachment to the tree trunk; au is the modulus of rupture of green wood. According to the field observation, the bur oak tree is the most common tree species in this area. For identified hazard trees, the parameters a_u, **d**, and **L** approximately have the following distributions: $a_u \sim InN(49.6MPa, 9.92 MPa), d \sim InN(0.lm, 0.05 m), and L$ InN(2.5m, 0.5 m), respectively. Although there may be more than one primary branch in a tree and more than one hazard tree along a power line, because it is very hard to determine the number of falling tree branches because of the limited knowledge of this complicated phenomenon, it is assumed only one tree branch falls on the midspan of a power line regardless of the real tree's location. **In** addition, the dynamic effect of falling trees is not considered due to the unavailability of data. For the purpose of demonstration, only the static load is applied to wires [44].

Considering that the geographical area covered by the studied distribution network is relatively small, it is assumed that the ice thickness, wind speed, and wind direction are the same throughout this area during an ice storm event [18]. Because of the unavailability of power demand data in winter, for the purpose of demonstration, the peak demand of customers during summer is used to calculate the power outage cost using Eq. (7). The unit cost of the lost load is assumed to be \$14/kWh [23]. The cost of replacing a wood pole is around \$3100, which includes the cost of materials, equipment, and labor [22]. The average tree trimming cost is around \$460 per tree. A simulation time step of 0.5 h is used so that the repair process of each failed component can be simulated accurately. The ice storm is assumed to hit the distribution network at the tenth hour of the simulation.

4.1. Resilience assessment without enhancement strategies

In this subsection, the ice storm resilience of the power distribution network without enhancement strategies is assessed. To assess the resilience of the power distribution network for a given ice storm scenario, first, given the ice thickness, wind speed, wind direction, and tree failures at each component site, component failures are evaluated according to component fragility models developed in Section 3; second, after removing the failed components, the performance of the power distribution network is evaluated with the system performance model introduced in Section 2; third, the power distribution network is restored by repairing failed components while considering recovery priority with the system restoration model introduced in Section 2. Firstly, five deterministic ice storm scenarios with different intensities (i. e., wind speed U and ice thickness ta but the same wind direction (0 = 22.5 m/s, t; = 1.9 cm), Case 3 (U = 22.5 m/s, t; = 2.5 cm), Case 4 (U = 20 m/s, t; = 2.5 cm), and Case 5 (U = 25 m/s, t; = 2.5 cm). The values of wind speed and ice thickness used in these scenarios are consistent with those with a 500-year mean recurrence interval specified in ASCE 7-16, as well as an ice storm that occurred in Oklahoma in October 2020 [6]. It is assumed that two repair teams are assigned to repair and recover the power distribution network. Restoration curves of the power distribution network for the five ice storm scenarios are shown in Fig. 9. Table 2 gives the resilience metrics of different ice storm scenarios, including the minimum network performance index Q,,,;,, resilience index RI, and restoration time 1R. Typically, the minimum network performance

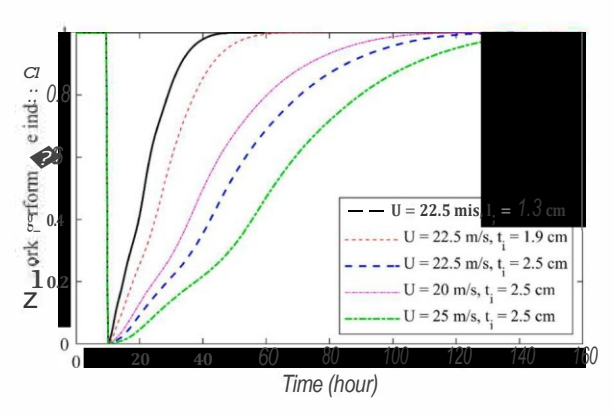


Fig. 9. Restoration curves for ice storms with different wind speeds and ice thicknesses (Cases 1 to 5, $0 = 90^{\circ}$).

 Table 2

 Resilience metrics of different cases.

Case	Ice storm scenario	n	Q,,	RI	TR (h)
1	$U = 22.5 \text{ m/s}, t = 1.3 \text{ cm}, 0 = 90^{\circ}$	2	0.01	0.82	38.5
2	$U = 22.5 \text{ m/s}, t_l = 1.9 \text{ cm}, U = 90^\circ$	2	0	0.74	55.5
3	$U = 22.5 \text{ m/S}, ti = 2.5 \text{ cm}, 0 = 90^{\circ}$	2	0	0.45	124
4	$U = 20 \text{ m/s}, t_1 = 2.5 \text{ cm}, 0 = 90^{\circ}$	2	0	0.54	108
5	$U = 25 \text{ m/s}, t = 2.5 \text{ cm}, 0 = 90^{\circ}$	2	0	0.31	150.5
6	$U = 25 \text{ m/s}, t = 1.9 \text{ cm}, 0 = 0^{\circ}$	2	0	0.73	65.5
7	$U = 25 \text{ m/s}, t, = 1.9 \text{ cm}, 0 = 30^{\circ}$	2	0	0.73	63
8	$U = 25 \text{ m/s}, t = 1.9 \text{ cm}, 0 = 60^{\circ}$	2	0	0.71	65
9	$U = 25 \text{ m/s}, t_l = 1.9 \text{ cm}, U = 90^\circ$	2	0	0.68	68.5
10	$U = 22.5 \text{ m/s}, t_t = 2.5 \text{ cm}, U = 90^{\circ}$	1	0	0.20	247
11	$U = 22.5 \text{ m/s}, ti = 2.5 \text{ cm}, 0 = 90^{\circ}$	3	0	0.61	83
12	$U = 22.5 \text{ m/s}, t_l = 2.5 \text{ cm}, U = 90^{\circ}$	4	0	0.70	62.5
13	$U = 22.5 \text{ m/s}, t_t = 2.5 \text{ cm}, U = 90^{\circ}$	5	0	0.76	50.5

index Q,,,in is reached immediately after the power distribution network is hit by an ice storm. In order to compare different ice storm scenarios, the control time for the period of interest tc is set as 72 h. Resilience index RI during the time period from 10 h to 82 h is obtained with Eq. (6). Restoration time 1R is the time needed for the power system to recover to the normal operation condition. By comparing Cases 1 to 3, it is found in Fig. 9 that the network performance decreases as the ice thickness increases. Meanwhile, as shown in Table 2, with the increase of the ice thickness, the resilience index RI decreases, and the restoration time 1R increases. For example, when the ice thickness increases from 1.9 cm in Case 2 to 2.5 cm in Case 3. RI decreases from 0.74 to 0.45, and 1R increase from 55.5 h to 124 h. Similarly, as shown in Fig. 9 and Table 2, the resilience of the power distribution network decreases with an increase in wind speed, in terms of decreased network performance index Q, resilience index RI, and increased restoration time 1R. Moreover, it is found that resilience reduction is nonlinear with respect to the increase in the ice storm intensity (i.e., ice thickness and wind speed). For example, as the wind speed increases from 20 m/s in Case 4 to 22.5 m/s in Case 3, the resilience index RI reduces by 17%. When the wind speed further increases to 25 m/s in Case 5, the resilience index RI reduces by 31%.

In order to gain more insight into how ice storms influence system resilience, it is necessary to know the distribution of different component failure modes. Fig. 10 gives the number of components with different failure modes for Cases 1 to 5. It is noted that Type 1 wire breakage refers to wind and ice-induced wire breakage while Type 2 wire breakage refers to tree and ice-induced wire breakage. It is found that short circuit is the most common failure mode. Short circuit accounts for more than 50% of the total failed components for all five cases and reaches as high as 99% for Case 1. This indicates that trees pose a significant risk to this power distribution network. Moreover, wire failure, including Type 1 wire breakage, Type 2 wire breakage, and short

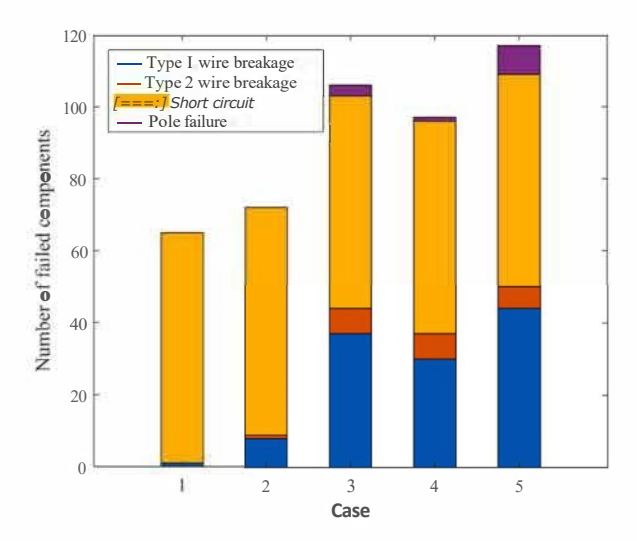


Fig. 10. Number of components with different failure modes.

circuit, accounts for more than 93% of the total failed components. In contrast, pole failure only accounts for less than 7%. This indicates that wires are more vulnerable than poles in this network. The number of Type 1 wire breakage increases with the increase in the ice thickness and wind speed. Type **2** wire breakage is affected mostly by the ice thickness. It is because higher ice thickness leads to higher tree damage probability, which further leads to a higher number of Type 2 wire breakage. The number of short circuits slightly changes with the ice storm intensity. This can be explained by the fact that as the ice thickness and wind speed increase, some wires switch the failure mode from short circuit to Type 1 or Type 2 wire breakage, although more wires begin to fail due to short circuit. Pole failure occurs at relatively high intensities. Although pole failure does not prevail, it can significantly deteriorate the network resilience, because it takes longer to replace a failed pole than repair the wire breakage and short circuit during the restoration process.

Next, four deterministic ice storm scenarios with the same intensity (U = 25 m/s, t; = 1.9 cm) but different directions are studied, which include Case 6 $(0 = 0^{\circ})$, Case 7 $(0 = 30^{\circ})$, Case 8 $(0 = 60^{\circ})$, and Case 9 $(0 = 90^{\circ})$. Fig. 11 presents the restoration curves for these four scenarios and Table 2 shows the resilience metrics. The resilience index of Case 6 $(0 = 0^{\circ})$ and 7 $(0 = 30^{\circ})$ are the same, and the highest among the four cases. Case 6 has higher network performance than Case 7 in the early recovery stage, but Case 7 has a faster restoration speed. As a result, the restoration time of Case 7 is shorter than Case 6. When the wind direction is equal to or larger than 30° for Cases 7 to 9, as the wind direction increases, both the network performance index and the

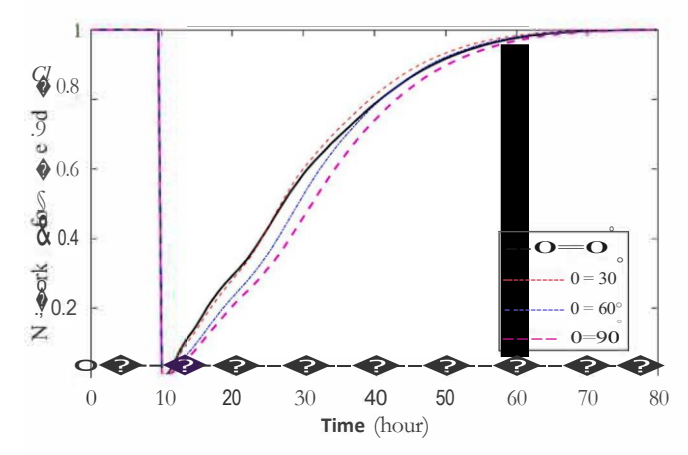


Fig. 11. Restoration curves for ice storms with different wind directions.

resilience index decrease, and the restoration time increases. As compared to the ice storm intensity, the effect of the wind direction on the resilience of the power distribution network is relatively limited. Although the maximum difference in resilience index between different wind direction cases is only 7%, the difference in power outage cost reaches as high as **19%**. This indicates that the effect of wind directions cannot be ignored.

Thirdly, the effect of recovery resources on the power distribution network resilience is investigated. Five cases with 1 to 5 repair teams for a deterministic ice storm scenario (U = 22.5 m/s, t; = 2.5 cm, $\theta = 90^\circ$) are studied, which include Case 10 (n = 1), Case 3 (n = 2), Case 11 (n = 3). Case 12 (n = 4), and Case 13 (n = 5). The restoration curves and resilience metrics of the five cases are presented in Fig. 12 and Table 2, respectively. It is observed that the resilience index RI increases and the restoration time TR decreases with the increase in the number of repair teams. Therefore, for an ice storm event, the resilience can be improved by increasing the repair teams, which is achieved by reducing the restoration time. It is also found that the improvement effect is more significant when the number of repair teams is relatively low. However, when there are sufficient resources, the improvement effect becomes less significant.

4.2. Resilience assessment with enhancement strategies

In this subsection, the ice storm resilience of the power distribution network with enhancement strategies is assessed and the costeffectiveness of different grid hardening strategies is investigated. The ice storm scenario with a wind speed of 22.5 m/s, wind direction of 90°, and ice thickness of 2.5 cm is used for the demonstration purpose. Three grid hardening strategies including upgrading poles (UP), vegetation management (VM), and both UP and VM (UP + VM) are studied and compared to the case without grid hardening strategies, which is called the baseline case. It is noted that Class 4 and 5 poles are replaced with Class 2 poles for the UP strategy in this study. The hardening budget is assumed to be \$100,000. Fig. 13 shows the restoration curves with different hardening strategies. Table 3 gives the results of different hardening strategies. It can be found that all three strategies can improve the resilience in terms of increased network performance index and decreased restoration time. Among the three hardening strategies, VM is the most effective, while UP is the least effective. The power outage cost is reduced by 28% with VM, whereas UP and UP + VM result in a 9% and 27% reduction in power outage cost, respectively.

In order to show the impact of the hardening budget on the power system resilience, a sensitivity analysis of power outage costs under different hardening budgets is performed. Fig. 14 shows the results of the sensitivity analysis. It is observed that the increase in the hardening budget leads to a reduction in power outage cost for all three hardening strategies. VM is the most cost-effective strategy for all budget cases. Moreover, it is found that the hardening efficiency becomes low with the

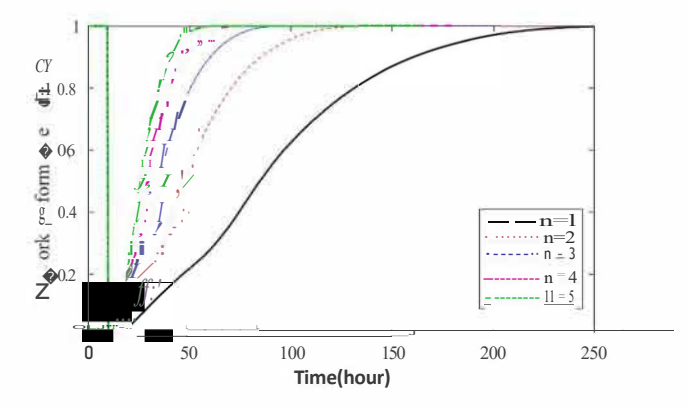


Fig. 12. Restoration curves with different number of repair teams.

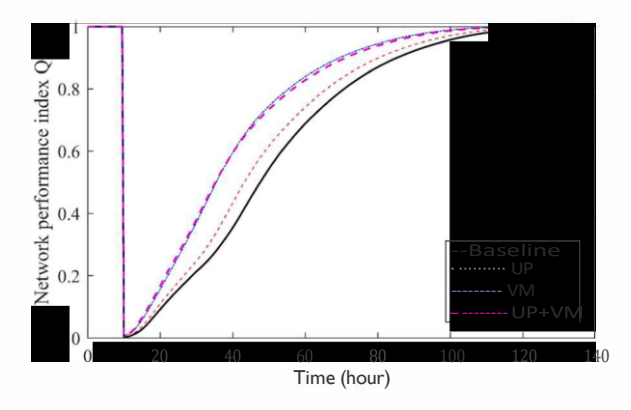


Fig. 13. Restoration curves with different hardening strategies.

Table 3
Results of different hardening strategies.

Strategies	Number of trimmed trees	Number of hardened poles	Hardening cost(\$)	Power outage cost (\$)	TR (h)
Baseline	0	0	0	733,727	124
UP	0	32	99,200	665,042	118
VM	216	0	99,360	530,597	108
UP+ VM	150	10	100,000	536,243	110

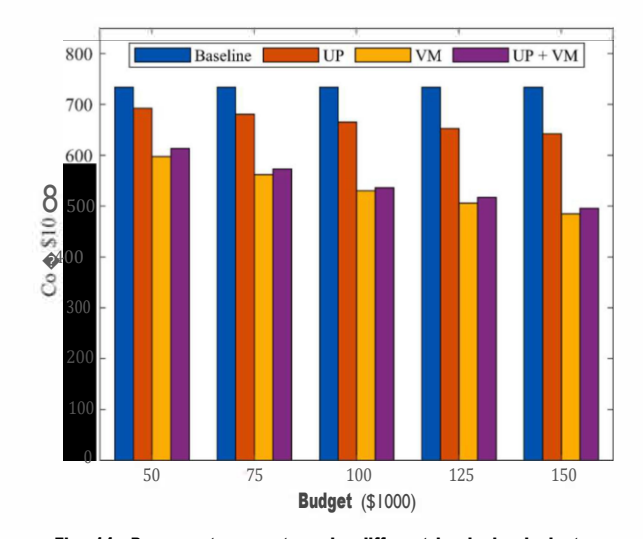


Fig. 14. Power outage costs under different hardening budgets.

increase in the hardening budget. For example, with the VM strategy, the power outage cost reduction increases by \$35,482 when the hardening budget increases from \$50,000 to \$75,000. However, when the hardening budget increases from \$125,000 to \$150,000, the power outage cost reduction only increases by \$20,721. This is because critical components with high $R\!A\!W$ values are given high hardening priority and further investment in non-critical components leads to low hardening efficiency.

5. Summary and conclusions

There have been limited studies on the ice storm resilience of power distribution systems. One main reason for this is that there are no available fragility models of distribution components subjected to ice storms. Most specifically, the fragility of tree-induced component damage during ice storms has not been studied, even if little such research has been conducted for hurricanes.

To address the aforementioned limitations, this paper presents a framework for assessing the resilience of power distribution systems subjected to ice storms and enhancing the system resilience with costeffective grid hardening strategies. This new framework includes five parts: ice storm characterization, component fragility models, power distribution system performance model, system restoration model, and resilience enhancement evaluation. As an important part of the framework, parameterized fragility curves of 3-span power pole-wire systems are developed utilizing finite element analysis and Monte Carlo simulation. Besides the pole failure, two more types of tree-induced wire failure modes overlooked in previous work are investigated by considering falling tree branches. In addition, tree damage fragility functions developed with tree damage data in a past ice storm event are employed to predict the tree damage probability. With these improvements, the tree-induced risk to power distribution systems can be assessed in a realistic way. Moreover, the vegetation management strategy that focuses on hazard trees can make the grid hardening more economical and cost-effective. The effectiveness of the framework is demonstrated through an application to a power distribution network in Oklahoma subjected to ice storms. In the application, the ice storm resilience is quantified with different metrics, and the effects of ice storm intensity, wind direction and recovery sources are investigated. Results show that system resilience decreases nonlinearly with respect to the increase in the ice storm intensity. It is found that the effect of wind directions cannot be ignored considering the significant increase in the outage cost caused by the most unfavorable wind direction. It is also found that resilience improvement can be achieved by increasing recovery resources. Furthermore, the cost-effectiveness of different grid hardening strategies is studied when there is a budget constraint. It should be noted that grid hardening strategies are highly dependent on network configurations and component vulnerabilities. Specific findings about grid hardening strategies developed in this example network may be different from other networks. This application highlights the capability of the proposed framework to quantify and enhance the resilience of power distribution systems subjected to ice storms.

In future work, the authors will continue to improve the proposed framework. For example, an ice storm model that can consider the moving speed of storms can be incorporated in order to evaluate the spatiotemporal impact of ice storms on the PDS component failures. The dynamic effect of falling trees can also be considered by determining the dynamic factor through falling tree tests. The number of falling tree branches during ice storm events needs to be quantified statistically when there are sufficient data. The effect of deterioration on the PDS component fragility will be incorporated.

CRediT authorship contribution statement

Guangyang Hou: Conceptualization, Methodology, Software, Investigation, Writing - original draft, Writing - review & editing. Kanthasamy K. Muraleetharan: Conceptualization, Writing - review & editing, Supervision, Project administration, Funding acquisition. Vinushika Panchalogaranjan: Conceptualization, Investigation, Writing - review & editing. Paul Moses: Conceptualization, Investigation, Writing - review & editing. Amir Javid: Conceptualization, Investigation, Writing - review & editing. Hussein Al-Dakheeli: Conceptualization, Investigation, Writing - review & editing. Rifat Bulut: Conceptualization, Investigation, Writing - review & editing. Richard Campos: Conceptualization, Investigation, Writing - review & editing. P. Scott Harvey: Conceptualization, Investigation, Writing review & editing. Gerald Miller: Conceptualization, Investigation, Writing - review & editing. Kirby Boldes: Conceptualization, Investigation, Writing - review & editing. Maha Narayanan: Conceptualization, Investigation, Writing - review & editing.

Declaration of Competing Interest

The authors declare that they have no known competing financial interests or personal relationships that could have appeared to influence the work reported in this paper.

Data Availability

Data will be made available on request.

Acknowledgments

This material is based on work supported by the National Science Foundation under Grant No. OIA-1946093. The authors would like to thank Nick Shumaker, Manager of System Engineering at the Oklahoma Electric Cooperative for his helpful cooperation in providing utility data for this analysis. Any opinions, findings, and conclusions or recommendations expressed in this paper are those of the authors and do not necessarily reflect the views of the National Science Foundation.

References

- Zou QL, Chen SR. Resilience modeling of interdependent traffic-electric power system subject to hurricanes. J Infrastruct Syst 2020;26:04019034.
- [2] Hines P, Apt J, Talukdar S. Large blackouts in North America: historical trends and policy implications. Energy Policy 2009;37:5249-59.
- [3] Shafieezadeh A, Onyewuchi PU, Begovic MM, DesRoches R. Fragility assessment of wood poles in power distribution networks against extreme wind hazards. Adv Hurric Eng Learn Our Past 2013:851-61.
- [4] Alam MM, Zhu ZB, Tokgoz BE, Zhang J, Hwang S. Automatic assessment and prediction of the resilience of utility poles using unmanned aerial vehicles and computer vision techniques. Int J Disaster Risk Sci 2020;11:119-32.
- [5] Kerry M, Kelk G, Etkin D, Burton I, Kalhok S. Glazed over: Canada copes with the ice storm of 1998. Environment 1999:41. 6-4.
- [6] Cooperative Electric Cooperative. October 2020 Ice storm leads to devastating damage across Oklahoma. 2020.
- [7] Bahrami A, Yan M, Shahidehpour M, Pandey S, Vukojevic A, Paaso EA. Mobile and portable de-icing devices for enhancing the distribution system resilience against ice storms: preventive strategies for damage control. IEEE Electrif Mag 2021;9: 120-9.
- [8] Ryan PC, Stewart MG, Spencer N, Li Y. Probabilistic analysis of climate change impacts on timber power pole networks. Int J Electr Power 2016;78:513-23.
- [9] Yan M, Shahidehpour M, Paaso A, Zhang L, Alabdulwahab A, Abusorrah A. Distribution system resilience in ice storms by optimal routing of mobile devices on congested roads. IEEE Trans Smart Grid 2020;12:1314-28.
- [10] Ryan PC, Stewart MG, Spencer N, Li Y. Reliability assessment of power pole infrastructure incorporating deterioration and network maintenance. Reliab Eng Syst Saf 2014:132:261-73.
- [11] Iannacone L, Sharma N, Tabandeh A, Gardoni P. Modeling time-varying reliability and resilience of deteriorating infrastructure. Reliab Eng Syst Saf 2022;217: 108074.
- [12] Ryan PC, Stewart MG. Cost-benefit analysis of climate change adaptation for power pole networks. Clim Change 2017;143:519-33.
- [13] Espinoza S, Panteli M, Mancarella P, Rudnick H. Multi-phase assessment and adaptation of power systems resilience to natural hazards. Electr Power Syst Res 2016;136:352-61.
- [14] Wang W, van de Lindt JW, Rosenheim N, Cutler H, Hartman B, Lee JS, et al. Effect of residential building wind retrofits on social and economic community-level resilience metrics. J Infrastruct Syst 2021;27. 04021034.
- [15] Wang W, van de Lindt JW. Quantitative modeling of residential building disaster recovery and effects of pre- and post-event policies. Int J Disaster Risk Res 2021;59: 102259.
- [16] Doom N, Gardoni P, Murphy C. A multidisciplinary definition and evaluation of resilience: the role of social justice in defining resilience. Sustain Resilient Infrastruct 2019;4:112-23.

- [17] Wu Y, Hou G, Chen S. Post-earthquake resilience assessment and long-term restoration prioritization of transportation network. Reliab Eng Syst Saf 2021;211: 107612.
- [18] Panteli M, Mancarella P. Influence of extreme weather and climate change on the resilience of power systems: Impacts and possible mitigation strategies. Electr Power Syst Res 2015;127:259-70.
- [19] Sharma N, Gardoni P. Mathematical modeling of interdependent infrastructure: an object-oriented approach for generalized network-system analysis. Reliab Eng Syst Saf 2022;217:108042.
- [20] Hughes W, Zhang W, Bagtzoglou AC, Wanik D, Pensado O, Yuan H, et al. Damage modeling framework for resilience hardening strategy for overhead power distribution systems. Reliab Eng Syst Saf 2021;207:107367.
- [21] Panteli M, Trakas DN, Mancarella P, Hatziargyriou ND. Power systems resilience assessment: hardening and smart operational enhancement strategies. Proc IEEE 2017;105;1202-13.
- [22] Salman AM, Li Y, Stewart MG. Evaluating system reliability and targeted hardening strategies of power distribution systems subjected to hurricanes. Reliab Eng Syst Saf 2015;144:319-33.
- [23] Ma SS, Chen BK, Wang ZY. Resilience enhancement strategy for distribution systems under extreme weather events. IEEE Trans Smart Grid 2018;9:1442-51.
- [24] Tari AN, Sepasian MS, Kenari MT. Resilience assessment and improvement of distribution networks against extreme weather events. Int J Electr Power 2021; 125:106414.
- [25] Canham CD, Papaik MJ, Latty EF. Interspecific variation in susceptibility to windthrow as a function of tree size and storm severity for northern temperate tree species. Can J For Res 2001;31:1-10.
- [26] Hou GY, Chen SR. Probabilistic modeling of disrupted infrastructures due to fallen trees subjected to extreme winds in urban community. Nat Hazards 2020;102: 1323-50
- [27] Gardoni P, Kiureghian AD, Mosalam KM. Probabilistic capacity models and fragility estimates for reinforced concrete columns based on experimental observations. J Eng Mech 2002;128:1024-38.
- [28] Dunn S, Wilkinson S, Alderson D, Fowler H, Galasso C. Fragility curves for assessing the resilience of electricity networks constructed from an extensive fault database. Nat Hazards Rev 2018;19:04017019.
- [29] Darestani YM, Shafieezadeh A. Multi-dimensional wind fragility functions for wood utility poles. Eng Struct 2019;183:937-48.
- [30] Shafieezadeh A, Onyewuchi UP, Begovic MM, DesRoches R. Age-dependent fragility models of utility wood poles in power distribution networks against extreme wind hazards. IEEE Trans Power Deliv 2014;29:131-9.
- [31] Yuan H, Zhang W, Zhu J, Bagtzoglou AC. Resilience assessment of overhead power distribution systems under strong winds for hardening prioritization. ASCE ASME J Risk Uncertain 2018;4:04018037.
- [32] Salman AM, Li Y. Age-dependent fragility and life-cycle cost analysis of wood and steel power distribution poles subjected to hurricanes. Struct Infrastruct Eng 2016; 12:890-903.
- [33] Park YJ, Glagola CR, Gurley KR, Son K. Performance assessment of the florida electric-power network system against hurricanes. Nat Hazards Rev 2014;15: 04014003.
- [34] Wang L. The fault causes of overhead lines in distribution network. In: Proceedings of the MATEC web of conferences. EDP Sciences; 2016. p. 02017.
- [35] Ouyang M, Duenas-Osorio L. Multi-dimensional hurricane resilience assessment of electric power systems. Struct Saf 2014;48:15-24.
- [36] Ren JZ, Song JY, Ellingwood BR. Reliability assessment framework of deteriorating reinforced concrete bridges subjected to earthquake and pier scour. Eng Struct 2021;239:112363.
- [37] Tabandeh A, Sharma N, Gardoni P. Uncertainty propagation in risk and resilience analysis of hierarchical systems. Reliab Eng Syst Saf 2022;219:108208.
- [38] ANSI-05.1. Wood poles specifications and dimensions. American National Standards Institute; 2017.
- [39] Trefinasa. Overhead conductors. Trefinasa; 2020.
- [40] IEEE. National electrical safety code (NESC)(R). Piscataway, NJ: IEEE; 2017. 2017.
- [41] Ausgrid. Network Standard NS220: Overhead design manual. 2011.
- [42] ASCE. Minimum design loads and associated criteria for buildings and other structures. Reston, VA: ASCE; 2016.
- [43] Pugsley AG. The gravity stiffness of a suspension-bridge cable. Q J Mech Appl Math 1952;5:385-94.
- [44] Lu Q, Zhang W. An integrated damage modeling and assessment framework for overhead power distribution systems considering tree-failure risks. Struct Infrastruct Eng 2022:1-16.